RESEARCH ARTICLE OPEN ACCESS

Synaptic Density in Multiple Sclerosis

An In Vivo Study Using [^{11}C]UCB-J-PET Imaging

Amelie Luoma,[1,2,3,4] Markus Matilainen,[1,2,3,4] Jouni Mikael Tuisku,[1,3] Richard Aarnio,[1,3] Taru Nikkilä,[2,3,4,5] Sini Laaksonen,[1,2,3,4] Mikko Koivumäki,[1,3] Eveliina Honkonen,[1,2,3,4] Marjo Nylund,[1,2,3,4] Saara Wahlroos,[1] Olof Solin,[1,6,7] Ming-Kai Chen,[8] Takuya Toyonaga,[8] Jussi Lehto,[1,3,4] Anniina Snellman,[1] Juha O. Rinne,[1,2,4] and Laura M. Airas[1,2,3,4]

Correspondence
Dr. Airas
laura.airas@utu.fi

Neurol Neuroimmunol Neuroinflamm 2025;12:e200435. doi:10.1212/NXI.0000000000200435

Abstract

Background and Objectives

Multiple sclerosis (MS) is a chronic inflammatory disease coupled with neurodegenerative processes affecting both the white matter and gray matter (GM) in the CNS. Several histopathologic studies have reported a reduction in synaptic density in various areas of the brain. However, this pathologic feature is yet an unexplored entity among people with MS (pwMS). Therefore, we sought to investigate synaptic loss in vivo by quantifying the synaptic vesicle glycoprotein 2A using [^{11}C]UCB-J-PET imaging and to explore associations with clinical and cognitive measures.

Methods

Ten pwMS and 8 healthy controls (HCs) underwent high-resolution [^{11}C]UCB-J-PET imaging and MRI. SV2A availability was determined using the tissue-to-plasma concentration ratio at equilibrium (distribution volume; V_T). We furthermore explored associations between PET imaging results and clinical and cognitive measures in pwMS (assessed with the Expanded Disability Status Scale (EDSS) and Symbol Digit Modalities Test [SDMT]). In addition, we considered volumetric, clinical, and cognitive measures during a 5-year period before PET imaging.

Results

Ten pwMS (7 women [70%], median [interquartile range] age, 53 [50–56]) years were compared with 8 HCs (6 women [75%]; age, 51 [50–70] years). PwMS had a significantly lower SV2A availability in the cortical GM (pwMS: mean [SD], V_T = 15.65 mL/cm^3 [2.26]; HCs: V_T = 18.14 mL/cm^3 [2.09]; p = 0.029, t test), as well as in several subcortical regions. Moreover, a lower SV2A availability in cortical GM correlated significantly with reduced SDMT values in pwMS (r = 0.071, p = 0.021; Spearman correlation coefficient). No association between physical disability (measured using EDSS) and SV2A availability was found.

Discussion

Using in vivo [^{11}C]UCB-J PET imaging, we provide evidence of reduced synaptic density in pwMS. Furthermore, the results reveal a link between synaptic loss and cognitive impairment. These findings highlight the potential of [^{11}C]UCB-J PET imaging as a promising tool for assessing clinically relevant aspects of GM pathology in MS.

MORE ONLINE

Supplementary Material

Introduction

Multiple sclerosis (MS) is a chronic inflammatory and neurodegenerative disease estimated to affect approximately 2.8 million people worldwide.[1] Pathologic changes in the CNS, involving both white matter (WM) and gray matter (GM), can lead to physical and cognitive impairment.

[1]Turku PET Centre, Turku University Hospital, University of Turku, and Åbo Akademi University, Turku, Finland; [2]Clinical Neurosciences, University of Turku, Turku, Finland; [3]InFLAMES Research Flagship, University of Turku, 20014 Turku, Finland; [4]Neurocenter, Turku University Hospital, Turku, Finland; [5]Psychology Services, Experts Services, Turku University Hospital, Turku, Finland; [6]Turku PET Centre, Accelerator Laboratory, Åbo Akademi University, Turku, Finland; [7]Department of Chemistry, University of Turku, Turku, Finland; [8]Department of Radiology and Biomedical Imaging, Yale University School of Medicine, New Haven, CT.

The Article Processing Charge was funded by the authors.

Glossary

EDSS = Expanded Disability Status Scale; **FLAIR** = fluid-attenuated inversion recovery; **GM** = gray matter; **HC** = healthy control; **IQR** = interquartile range; **MS** = Multiple Sclerosis; **PF %** = Parenchymal Fraction; **PVE** = partial volume effect; **pwMS** = people with MS; **ROI** = regions of interest; **SDMT** = Symbol Digit Modalities Test; **TAC** = time-activity curve; **VT** = distribution volume; **VTR** = Finnish Governmental Research Funding; **WM** = white matter.

Despite its early recognition[2] and high prevalence,[3] neuropsychological dysfunction remains an insufficiently understood aspect of MS that is yet lacking effective treatment.[4] GM alterations, such as focal lesions, loss of synapses, and the associated atrophy, likely play a role in the development of cognitive impairment in MS because they have demonstrated predictive value for the degree of disability.[5]

To date, evidence supporting synaptic loss in people with MS (pwMS) is based on a relatively small number of human postmortem studies,[6] which have demonstrated a lower synaptic density in various parts of the CNS, such as in the cortex,[7] thalamus,[8] hippocampus,[9] cerebellum,[10] and spinal cord.[11] Synaptic loss, although primarily reported from lesional GM areas, was also found in normal-appearing GM.[6] Yet, postmortem studies have obvious limitations in correlating histologic and clinical findings.

A recently introduced approach uses the PET tracer [^{11}C]UCB-J (eFigure 1) to visualize the synaptic vesicle protein 2A (SV2A) in vivo.[12] Among the 3 known isoforms of the synaptic vesicle protein 2 (SV2A, SV2B, and SV2C), SV2A is the only ubiquitously expressed isoform throughout the chemical synapses of the adult brain.[13] This qualifies it to be a suitable target for the analysis of synaptic density. Moreover, [^{11}C]UCB-J has demonstrated high specificity and sensitivity in detecting SV2A, as well as good test-retest reproducibility.[12,14]

The aims of this study were to examine the density of SV2A in pwMS compared with healthy controls (HCs) in vivo and to explore the relationships between SV2A availability and cognitive disability and other clinical and radiologic characteristics. We hypothesized reduced SV2A availability in pwMS compared with HCs.

Methods

Standard Protocol Approvals, Registrations, and Patient Consents

The study was performed as a clinical PET and MRI study at the Turku PET Centre. The study protocol was approved by the ethics committee of the well-being services county of Southwest Finland (Dnro: 19/1801/2016), and written informed consent was obtained from all participants before participation in the study. The study was conducted according to the principles of the Declaration of Helsinki.

PwMS were examined with MRI and clinical and cognitive assessments between 2016 and 2017 as part of a clinical trial NCT03134716, the aim of which was to elucidate factors predisposing pwMS for later progression. For the original trial NCT03134716, the main inclusion criteria were a definite MS diagnosis for more than 5 years before enrollment and age between 40 and 55 years. Exclusion criteria were relapse or corticosteroid treatment within 30 days of evaluation both at the time of the PET imaging as well as 5 years earlier, an active neurologic or autoimmune disease other than MS, another comorbidity considered significant, pregnancy, or breastfeeding. The present cohort consists of 10 pwMS who had participated in the trial NCT03134716, who exhibited none of the exclusion criteria, and who consented to participation in the present study. These trial participants were then reimaged with MRI and additional [^{11}C]UCB-J-PET for synaptic density and reassessed for clinical and cognitive parameters between 2021 and 2022 (Figure 1). In addition, 8 HCs underwent MRI and [^{11}C]UCB-J-PET imaging. Exclusion criteria for HCs were a neurologic or psychiatric disease affecting the CNS, as well as pregnancy or breastfeeding.

Data Acquisition During 2016–2017

Participants underwent cranial MRI with a 3T scanner (Philips Ingenuity [PET]/MR System) and T1 and fluid-attenuated inversion recovery (FLAIR)-weighted images were acquired. Furthermore, clinical and cognitive examinations using Expanded Disability Status Scale (EDSS) and Symbol Digit Modalities Test (SDMT) as a measure of processing speed, respectively, was performed.

Data Acquisition During 2020–2023

PET Imaging, MRI, and Clinical Evaluation

Participants had a [^{11}C]UCB-J-PET scan and cranial MRI. PET scans were performed on a high-resolution research tomograph (HRRT; Siemens) with a reconstructed image resolution of 2.5 mm. Thermoplastic heat masks were used during imaging. The PET data were reconstructed using 3D ordinary Poisson ordered subset expectation maximization (OP-OSEM) point spread function reconstruction, which provides partial volume effect (PVE) correction, improves the spatial resolution, and is independent of the assumptions of postreconstruction PVE correction methods.[15] T1-weighted and FLAIR-weighted MR images were acquired on a 3T scanner (Philips Ingenia). For attenuation correction, a 6-minute transmission scan was performed before every [^{11}C]UCB-J injection. Simultaneously with an IV bolus injection of the tracer, 90 minutes of dynamic PET imaging was initiated. PET images of participants were reconstructed in 29 frames

Figure 1 Study Timeline

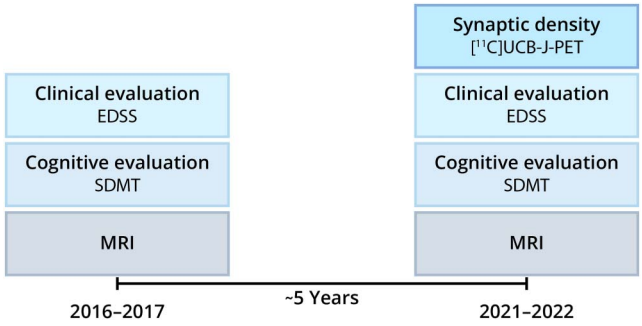

Illustration of the study time line for pwMS. All pwMS underwent MRI, clinical, and cognitive evaluation between 2016 and 2017. After approximately 5 years, between 2021 and 2022, these examinations were repeated and participants additionally underwent [^{11}C]UCB-J-PET imaging to determine synaptic density. pwMS = people with multiple sclerosis.

(6 × 30 seconds, 7 × 60 seconds, and 16 × 300 seconds).[16] After reconstruction, the data were smoothed using a Gaussian 2.5 mm full width at half maximum postreconstruction filter. For pwMS, clinical and cognitive examinations using EDSS and SDMT, respectively, were performed.

Radiosynthesis of [^{11}C]UCB-J

For the radiosynthesis of [^{11}C]UCB-J, we modified previously published[12,16-19] procedures; acid pretreatment of the boronated precursor was performed with a stronger acid (30% HCl), the handling of reactants in the synthesis device was optimized to be better amenable for automation, and the protocol for HPLC separation of the product was optimized. Details about our radiosynthesis are given in the supplemental materials (eMethods).

Blood Analysis

All participants underwent arterial cannulation. Blood samples were collected to analyze the plasma time-activity curve (TAC) and to perform radiometabolite analysis for determining the unmetabolized fraction (i.e., parent fraction) of [^{11}C]UCB-J in plasma. Details about our blood analysis are given in the supplemental materials (eMethods, eTable1).

Postprocessing and Analysis of PET and MR Images

Arterial plasma activities were converted to blood, with an average plasma-to-blood ratio curve based on samples of 7 participants. The radiometabolite corrected arterial input curve was created as follows. A monoexponential function

$$f(x) = (A - B)e^{-Cx} + B \quad (1)$$

where A = 1, B ≥ 0, C > 0, was fitted to each individual's parent fraction measurements, after which the radiometabolite corrected plasma TACs were calculated by multiplying the uncorrected plasma curves with the estimated model curve. The differences in appearance times of radioactivity between PET and arterial plasma TACs were corrected by first estimating the delay of the arterial plasma TAC, which produced the best fit of the one-tissue compartment model to whole-brain TAC and then shifting the arterial plasma TAC accordingly. The 1TCM was selected for the final data analysis, similarly as documented by others.[14,20]

PET data were preprocessed using an integrated brain image processing pipeline (MAGIA pipeline[21]), which includes motion correction, coregistration of MR and PET images, and automated delineation of regions of interest (ROIs). For the segmentation of MR images, FreeSurfer software version 7.2.0[22] was applied. During preprocessing, PET data were interpolated to MR 1× 1 ×1 mm^3 resolution to match with the segmented MS lesion images. Furthermore, the voxel-level parametric distribution volume (V_T) images were estimated using plasma input Logan method in a 40–90-minute time interval, where the dynamic PET data were smoothed using 4 mm full width at half maximum Gaussian filter before modeling.

T1 and T2 lesion masks were created from MRI, with T2 lesion masks based on FLAIR images. As a first step, a semiautomated method using the Lesion Segmentation Tool was applied.[23] Thereafter, each slice was manually edited using Carimas, as previously described.[24] For the segmentation of MRI images, FreeSurfer software version 7.2.0[22] was applied. Volumes of different ROIs were calculated from these FreeSurfer-based masks and T1 and T2 volumes were calculated from the lesion masks. Normal-appearing WM (NAWM) was defined as WM minus T2 lesions.

For regional quantification, several ROIs were selected. Of primary interest was the cortical GM, which was further analyzed with the following FreeSurfer-given subregions: cingulate cortex, frontal cortex, insular cortex, occipital cortex, parietal cortex, and temporal cortex. Furthermore, the following exploratory ROIs were defined: amygdala, caudate nucleus, cerebellum, hippocampus, putamen, thalamus, and NAWM. Regional V_Ts were estimated using the one-tissue compartment model using a radiometabolite-corrected arterial plasma input curve and blood input curve, where the blood volume fraction was fixed at 5%. We chose this method because it is independent from WM (centrum semiovale) as a reference, which is of importance because especially the WM is highly affected by alterations in MS.

V_T values of pwMS and HCs were compared in all ROIs. Furthermore, correlations between SV2A availability and various radiologic and clinical parameters were explored in primary regions. These included GM volume parenchymal fraction (PF, %) at the time of the PET imaging, GM volume change (%), disease duration since diagnosis at the time of PET imaging, SDMT at the time of PET imaging, SDMT change, EDSS at the time of PET imaging, and EDSS change. Furthermore, the relations between volumetric data and

clinical parameters were investigated in primary regions. In addition, the correlation between SV2A availability in exploratory regions and cognitive measures (SDMT at the time of PET imaging and SDMT change) were investigated.

Statistical Analysis

Statistical analysis was performed using R (version 4.2.1). Fisher exact test was used to compare the gender distributions between HCs and pwMS. Continuous variables were assessed using the independent samples *t* test or Wilcoxon rank sum test (HCs vs pwMS) and 1-sample *t* test or Wilcoxon rank sum test (change). Normality of the variables was checked using Shapiro-Wilk test. In Table 1, the *t* test was used for variables with mean (SD) and Wilcoxon test for variables with median and interquartile range (IQR). V_T values of defined ROIs between pwMS and HCs were compared with the independent samples *t* test or Wilcoxon rank sum test, depending on the normality of the variable. In addition, for cortical subregions, the results with multiple comparison correction false discovery rate (FDR) are also presented.

Pearson or Spearman correlation coefficients were used to evaluate the relationships between continuous variables, depending on the normality of the variables. FDR was additionally used over all primary subregion correlations with SDMT and SDMT change. Stepwise linear regression was used to assess if age, sex, or ROI's own volume (as PF, %) could be used as predictors for V_T of SV2A availability. Model building started with group factor (MS vs HCs) only, followed by the other variables. Akaike information criterion was used to test whether each variable would improve the model fit significantly. The final model included all those variables that significantly improved the model. Where model assumptions were violated, results were confirmed using log variable transformation. All tests were 2-tailed. Results with a p value <0.05 were considered significant. Variables are reported as mean (SD), unless otherwise stated.

Data Availability

On reasonable request, details of the analysis and participants will be shared anonymized.

Results

Demographic, Radiologic, and Cognitive Characteristics

PwMS did not differ from HCs in terms of sex, age, and radiation dosage (p = 1.0, p = 1.0, and p = 0.3, respectively; Table 1). Moreover, there were no differences observed when comparing the brain volume PF (%) (p = 0.14), NAWM volume PF (%) (p = 0.3), thalamus volume PF (%) (p = 0.091), and cortical GM volume PF (%) (p = 0.067) between pwMS and HCs (Figure 2).

Of 10 pwMS, 7 had relapsing-remitting MS, while 3 had secondary progressive MS at the time of PET imaging. The median (IQR) time since diagnosis was 16.0 years (12–20) and the median EDSS was 3.25 (3.0–4.0). Between the initial MRI and PET imaging 5 years later, the EDSS changed by 0.5 (0.12–1.0) (median [IQR]) points (p = 0.021). The mean [SD] SDMT value of all pwMS was 49 [16] at the time of PET imaging, while the mean [SD] SDMT change during the 5 previous years was −5.5 [8.5] (p = 0.072). The SDMT change ranged from −17 to 7. Seven pwMS had a decrease in SDMT values over 5 years, with a minimum of 12 points in 4 individuals. At the time of the second MRI and PET imaging, the median [IQR] WM T1 lesion volume was 3.0 cm^3 [1.1–4.4] and the median T2 lesion volume was 5.6 cm^3 [3.6–8.2]. During the 5 years between the initial MR imaging and the time of second MRI and PET imaging, the T1 lesion volume increased by 0.25 cm^3 [0.13–0.45] (median [IQR]) (p = 0.002) and the T2 lesion volume enlarged by 0.32 cm^3 [0.12–1.4] (p = 0.049).

Furthermore, during the 5 years, the cortical GM volume PF (%) and NAWM volume PF (%) reduced in pwMS on average by −1.8 (0.51) (p < 0.001) and −0.66 (0.78) (p = 0.025), respectively. While the brain volume PF (%) decreased by −2.6 (0.76) (p < 0.001), the thalamus volume PF (%) changed by −0.04 (0.05) (PF [%]; p = 0.022).

Additional demographic information of pwMS is given in the supplementary material (eTable 2).

SV2A Availability in pwMS and HCs

Primary Cortical GM Regions

SV2A availability was lower (13.7%) in cortical GM in pwMS (V_T = 15.65 mL/cm^3 [2.26]) compared with HCs (V_T = 18.14 mL/cm^3 [2.09]); p = 0.029; (Figure 3A, Table 2). Furthermore, SV2A availability was lower in all cortical subregions compared with HCs. The greatest difference of 15.2% was observed in the temporal cortex (V_T = 15.65 mL/cm^3 [2.22] in pwMS vs V_T = 18.46 mL/cm^3 [2.40] in HCs; p = 0.024), followed by the insular, occipital, cingulate, frontal, and parietal cortices (relative difference ranging from 15.0% to 12.9%; p values ranging from p = 0.021 to p = 0.038). In all cortical subregions, the significance of the reduction of SV2A availability survived FDR correction (p = 0.038 for all after correction). Furthermore, compared with HCs, in pwMS, a lower SV2A availability in cortical GM (p = 0.023) and all cortical subregions, except the parietal cortex, was seen after the application of a linear regression model (Table 2).

Exploratory Regions

A difference in SV2A availability in the amygdala, putamen, and thalamus was observed in pwMS compared with HCs (V_T = 15.34 mL/cm^3 [1.95] vs V_T = 17.56 mL/cm^3 [2.48]; p = 0.034; V_T = 17.03 mL/cm^3 [2.08] vs V_T = 19.88 mL/cm^3 [3.13]; p = 0.048; and V_T = 10.67 mL/cm^3 [1.64] vs V_T = 12.44 mL/cm^3 [1.55]; p = 0.033, respectively; Table 2). Four exploratory regions (including caudate nucleus [p = 0.059], cerebellum [p = 0.24], hippocampus [p = 0.36], and NAWM [p = 0.44]) showed no difference when comparing pwMS and HCs. After applying a linear regression model, lower SV2A availability in pwMS compared with HCs was confirmed in

Table 1 Demographic Information and Group Comparison of Participants

	HC (n = 8)	MS (n = 10)	HC vs MS (*p* value)	MS: change compared with 5 y ago	Change *p* value
Female, N (%)	6 (75)	7 (70)	1		
RRMS/SPMS, N (%)		7 (70)/3 (30)		−3/+3	
Age (y)	51 (50–70)	53 (50–56)	1		
Years since diagnosis (y)		16 (12–20)			
EDSS		3.25 (3.0–4.0)		0.5 (0.12–1)	0.021
SDMT, mean (SD)		49 (16)		−5.5 (8.5)	0.072
Brain volume PF (%), mean (SD)	86 (3.9)	82 (5.0)	0.14	−2.6 (0.76)	< 0.001
NAWM volume PF (%), mean (SD)	35 (3.0)	33 (4.1)	0.3	−0.66 (0.78)	0.025
Cortical GM volume PF (%), mean (SD)	32 (1.4)	30 (2.0)	0.067	−1.8 (0.51)	<0.001
Thalamus volume PF (%), mean (SD)	1.09 (0.10)	1.0 (0.1)	0.091	−0.04 (0.05)	0.022
T1 lesion volume (cm^3)		3.0 (1.1–4.4)		0.25 (0.13–0.45)	0.002
T2 lesion volume (cm^3)		5.6 (3.6–8.2)		0.32 (0.12–1.4)	0.049
Radiation dosage (MBq)	497 (487–501)	485 (402–499)	0.3		

Abbreviation: EDSS = Expanded Disability Status Scale; GM = gray matter; HC = healthy control; IQR = interquartile range; MBq = megabecquerel; MS = multiple sclerosis; NAWM = normal-appearing white matter; PF = parenchymal fraction; SDMT = Symbol Digit Modalities Test.
Values as median (IQR) unless otherwise specified. *P* values for continuous variables were calculated using the independent samples *t* test or Wilcoxon rank sum test (HC vs MS) and 1-sample *t* test or Wilcoxon rank sum test (change). *t* Tests were used for variables with mean (SD), Wilcoxon tests for variables with median (IQR), and Fisher exact test for sex. If not otherwise stated, data refer to the time point of the PET imaging (end of follow-up).

the amygdala ($p = 0.005$), putamen ($p = 0.034$), and thalamus ($p = 0.025$) (Figure 3A).

Associations Between Information Processing Speed and SV2A Availability

Primary Cortical GM Regions

V_T values in the cortical GM correlated with SDMT scores at the time of [^{11}C]UCB-J-PET imaging ($r = 0.71$, $p = 0.021$, Figure 4A, Table 3). Furthermore, V_T values in all cortical subregions correlated with SDMT scores obtained at the time of PET imaging (ranging from $r = 0.69$ to $r = 0.75$ and $p = 0.012$ to $p = 0.027$).

Lower cortical GM V_T values correlated with a decrease in SDMT scores over a 5-year period ($r = 0.71$, $p = 0.021$; Figure 4). Moreover, a correlation between lower V_T values and a negative SDMT score change in all cortical subregions was observed (ranging from $r = 0.64$ to $r = 0.76$ and $p = 0.011$ to $p = 0.046$). For primary subregions, all SDMT and SDMT change correlations survived correction for multiplicity.

Exploratory Regions

A correlation between V_T values in the amygdala, caudate nucleus, cerebellum, and hippocampus and SDMT scores at the time of [^{11}C]UCB-J- PET imaging was found ($r = 0.76$, $p = 0.011$; $r = 0.74$, $p = 0.015$; $r = 0.74$; $p = 0.015$, and $r = 0.68$, $p = 0.029$, respectively; Table 3). V_T values of the putamen and thalamus did not significantly correlate with SDMT scores at the time of the PET imaging. Furthermore, a correlation between V_T values of the amygdala, caudate nucleus, hippocampus, putamen, and thalamus and SDMT score change during the 5 years preceding the PET imaging was found ($r = 0.75$, $p = 0.013$; $r = 0.69$, $p = 0.027$; $r = 0.72$; $p = 0.020$, $r = 0.63$, $p = 0.049$, and $r = 0.75$, $p = 0.013$, respectively). V_T values of the cerebellum did not significantly correlate with the SDMT score alterations. No correlations were seen between V_T values of the NAWM and SDMT scores (data not shown).

Association Between SV2A Availability in Primary Cortical GM Regions and Radiologic and Clinical Measures Among pwMS

Clinical Measures

Cortical SV2A availability did not correlate with disease duration or EDSS at the time of PET imaging, nor with EDSS change during the 5-year period preceding the PET imaging (eTable 3). Furthermore, the SV2A availability in none of the cortical subregions correlated with disease duration or EDSS at the time of PET imaging, nor EDSS change during the 5 years preceding the PET imaging (data now shown).

A correlation was observed between EDSS points and SDMT scores at the time of PET imaging in pwMS ($\rho = -0.64$, $p = 0.048$; Figure 4B).

Radiologic Measures

Cortical SV2A availability did not correlate with GM volume PF (%) at the time of PET imaging, nor with GM volume PF

Figure 2 Comparison of Cortical GM Volume of pwMS and HCs

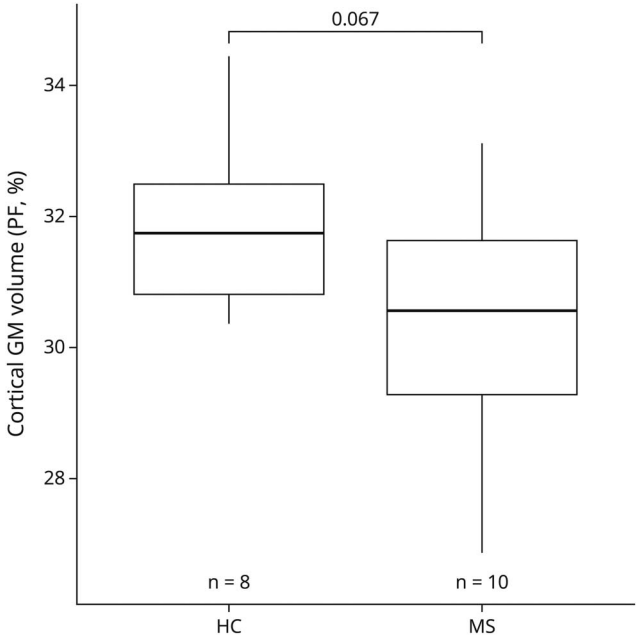

Box plots illustrating the cortical GM volume of pwMS and HCs. While the mean (SD) cortical GM volume (PF %) of pwMS was with 30 (2.0), slightly lower than the cortical GM volume of HCs with 32 (1.4), this difference was not statistically significant. T test was applied for comparison. GM = gray matter; HC = healthy control; MS = multiple sclerosis; PF % = parenchymal fraction; pwMS = people with multiple sclerosis.

change (%) during the 5 years preceding the PET imaging (eTable 3). Furthermore, the SV2A availability of none of the cortical subregions correlated with the GM volume PF (%) at the time of PET imaging, nor with GM volume PF change (%) during the 5 years preceding the PET imaging (data not shown).

Discussion

The main objective of this study was to compare SV2A availability as a measure of synaptic density between pwMS and HCs using [^{11}C]UCB-J PET imaging. The region of primary interest in this study was the cortical GM, in which our results suggest a lower synaptic density of approximately 14% in pwMS compared with HCs. Furthermore, we report an association between impairment in information processing speed measured with SDMT and reduced cortical synaptic density.

Several postmortem studies have examined the synaptic density in pwMS,[6] while our study represents a comparable in vivo investigation. Of 6 postmortem studies, which have examined the synaptic density in various cortical areas,[6] 3 report a reduction of approximately 50% in the synaptic density in the lesional GM cortex.[7,25,26] Two studies provide further evidence for lesion-independent synaptic loss in normal-appearing GM of the cortex, albeit to a smaller degree than in lesional GM.[7,26] Two other studies report no overall reduction in the synaptic density in cortical areas but found focal synaptic loss in colocation with activated microglia.[27,28]

In addition, we examined the synaptic density in 6 exploratory GM regions, namely amygdala, caudate nucleus, cerebellum, hippocampus, putamen, and thalamus. In line with our results, synaptic loss has been reported in the thalamus in MS brain in postmortem histology analyses and in animal models of MS.[8,26] Our results showed no significant synaptic loss in the cerebellum and hippocampus in pwMS, and indeed, histopathologic examinations present inconsistent results in those areas. A previous study[10] provided evidence for presynaptic loss in the dentate nucleus, while 2 other studies did not find a lower synapse number in the cerebellum.[29,30] On the other hand, 3 studies reported a reduced synaptic density in the hippocampus[31-33]; however, the decrease was partly limited to hippocampal subregions.[31] All in all, there seems to be significant regional heterogeneity of synaptic density and SV2A availability.[34]

Synaptic loss in pwMS, as assessed with [^{11}C]UCB-J PET imaging, is less pronounced compared with findings in histopathologic studies. In comparison with other studies that have used the tracer [^{11}C]UCB-J to assess synaptic density in other CNS conditions, our results are comparable with diseases such as schizophrenia with a synaptic loss of 10%–15% in various cortical areas and the hippocampus[35]; major depressive disorder, which has shown approximately 15% reduction in the dorsolateral prefrontal cortex, anterior cingulate cortex, and hippocampus[36]; as well as cannabis use disorder, which leads to approximately 10% synaptic loss in the hippocampus.[37] On the other hand, various neurodegenerative diseases have shown higher synaptic loss, such as Alzheimer disease with over 40% reduction in the hippocampus[38] and Parkinson disease with up to 35% reduction in the substantia nigra.[39,40]

The loss of chemical synapses in MS likely takes place in the context of a complex disease pathology affecting the entire CNS. With this study, we could show that a lower synaptic density is not limited to a specific brain region in MS, but rather affects a wide range of areas. Moreover, our findings indicate wide interindividual heterogeneity in synaptic density, which is not surprising considering the wide variety of clinical and neuropathologic presentations associated with MS. Synaptic loss is part of GM pathology, which is furthermore characterized by demyelination, neuronal and axonal loss, as well as transected dendrites.[25,41] A lower synaptic density is often considered to be a consequence of secondary degeneration; however, the decrease of the synaptic density seems to be partly independent of axonal loss,[7] and additionally, it can be observed in normal-appearing GM.[7,26] This gives rise to the question of a primary process leading to synaptic loss in MS, exceeding secondary degeneration. In our study, this hypothesis is supported by the relatively low level

Table 2 Synaptic Vesicle Glycoprotein 2A PET Outcome Measures (V_T) in Brain Regions of Interest

Region of interest	HC (n = 8)	MS (n = 10)	Relative difference (%)	*p* Value (FDR adjusted for subregions)	*p* Value after modelling
Primary regions					
Cortical GM	18.14 (2.09)	15.65 (2.26)	−13.7	0.029	0.023[a]
Cingulate cortex	19.13 (2.11)	16.52 (2.55)	−13.6	0.031 (0.038)	0.034
Frontal cortex	17.87 (2.11)	15.47 (2.22)	−13.4	0.033 (0.038)	0.025[a]
Insular cortex	18.64 (2.80)	15.85 (2.21)	−15.0	0.038 (0.038)	0.023[a]
Occipital cortex	18.08 (2.00)	15.43 (2.39)	−14.7	0.021 (0.038)	0.023
Parietal cortex	18.48 (1.88)	16.09 (2.38)	−12.9	0.030 (0.038)	0.075[b]
Temporal cortex	18.46 (2.40)	15.65 (2.23)	−15.2	0.023 (0.038)	0.016[a]
Exploratory regions					
Amygdala	17.56 (2.48)	15.04 (1.95)	−14.4	0.034[d]	0.005[a,b]
Caudate nucleus	17.40 (2.43)	15.04 (2.45)	−13.6	0.059	0.082[a,b]
Cerebellum	12.81 (1.81)	11.07 (2.13)	−13.6	0.24[d]	0.084
Hippocampus	13.18 (1.75)	11.57 (1.68)	−12.2	0.36[d]	0.050[a]
Putamen	19.88 (3.13)	17.03 (2.08)	−14.3	0.048	0.034
Thalamus	12.44 (1.55)	10.67 (1.64)	−14.2	0.033	0.025[a]
NAWM	8.34 (1.00)	7.98 (0.92)	−4.3	0.44	0.18[c]

Abbreviations: FDR = false discovery rate; GM = gray matter; HC = healthy control; MS = multiple sclerosis; NAWM = normal-appearing white matter; V_T = distribution volume.
Values are as mean (SD) V_T (mL/cm^3). Crude *p* values are from independent samples *t* test. For primary subregions, FDR-corrected *p* values are given in brackets. No multiple comparison correction was performed for exploratory regions. *p* Values after stepwise linear regression modelling are reporting on V_T differences between HC and MS groups when considering the impact of adjusting variables (sex, volume of the region and age) on V_T. The adjusting variables were added to the model only if they made the model better according to Akaike information criterion, compared with a simpler model. Because model assumptions were violated in several models, the significant results were confirmed with log(V_T) values.
[a] Sex was added to the model.
[b] Volume of the region was added to the model.
[c] Age was added to the model.
[d] Wilcoxon rank sum test used because of non-normality.

of atrophy in pwMS. Furthermore, synaptic density in cortical areas seemed not to be directly associated with the GM volume nor GM volume change. Another pathologic factor driving cortical synaptic loss might be meningeal B-cell follicles that may excrete proinflammatory and neurotoxic factors directly affecting the nearby cortex.[30,42] Therapeutic efforts modulating or depleting the meningeal B-cell follicles or promoting remyelination may thus reduce synaptic loss, now quantifiable using [^{11}C]UCB-J PET imaging.

On the other hand, our data suggest that synaptic loss is directly involved in pathologic mechanisms leading to cognitive dysfunction in MS. We assessed the cognitive ability using SDMT, which is primarily a measure for the information processing speed, representing the amount of information that an individual can process in a set time span.[43] An impairment in information processing speed is a characteristic cognitive feature among pwMS and has been described in a large proportion of patients.[44,45] Furthermore, a decrease in SDMT performance has shown to be associated with employment status and activities of daily living.[46-48] The magnitude of change in SDMT points demonstrating a clinically meaningful decline in information processing speed is, however, still being discussed.[49] Neuronal networks that are activated during the SDMT testing include regions of the frontoparietal attentional network, occipital cortex, precuneus and cuneus, as well as cerebellum.[50] Furthermore, in our cohort, synaptic density seemed to be more robustly correlated with impairment in processing speed than brain atrophy, which has shown to be of predictive value for cognitive decline in previous studies.[3,51]

We provide evidence that [^{11}C]UCB-J PET imaging can be used to measure alterations in synaptic density in pwMS. Considering the need for novel imaging techniques to visualize MS progression-related pathology in vivo, our data suggest [^{11}C]UCB-J PET imaging to be a promising approach to monitor mechanisms behind cognitive disability progression and to provide novel measures for clinical trials addressing neurocognitive dysfunction in MS.

Figure 3 Comparison of [^{11}C]UCB-J Availability in Various Brain Regions of Interest Between pwMS and HCs

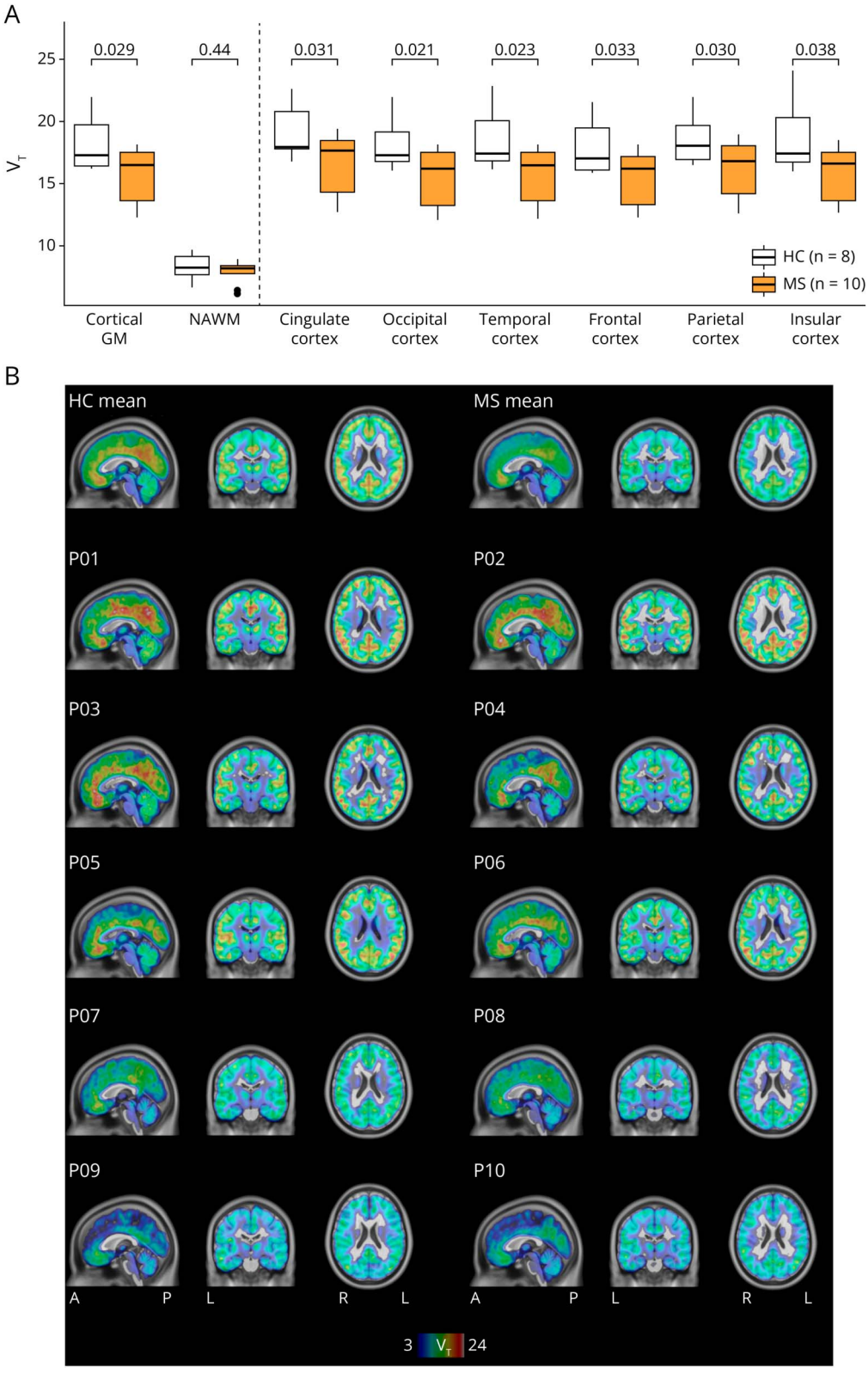

(A) Mean (SD) V_T (mL/cm^3) values of primary cortical GM regions and the NAWM. Significantly lower V_T values in cortical GM as well as in all cortical subregions are seen in pwMS in comparison with HCs, whereas no difference can be observed in the NAWM. *p* Values are from independent samples *t* test. (B) Illustration of the difference in [^{11}C]UCB-J availability between the HC mean and MS mean (top row). Parametric images for each patient visualize the interindividual heterogeneity in the radioligand binding. The color bar describes the dynamic range of the [^{11}C]UCB-J volume of distribution. Brighter orange indicates higher synaptic density. The parametric V_T images were estimated using plasma input Logan method in a 40–90-minute time interval, where the dynamic PET data were smoothed using a 4 mm FWHM Gaussian filter before modeling. FWHM = full width at half maximum; GM = gray matter; HC = healthy control; MS = multiple sclerosis; NAWM = normal-appearing white matter; pwMS = people with MS.

Figure 4 Correlations Between SV2A Availability in Cortical GM and Cognitive and Clinical Measures

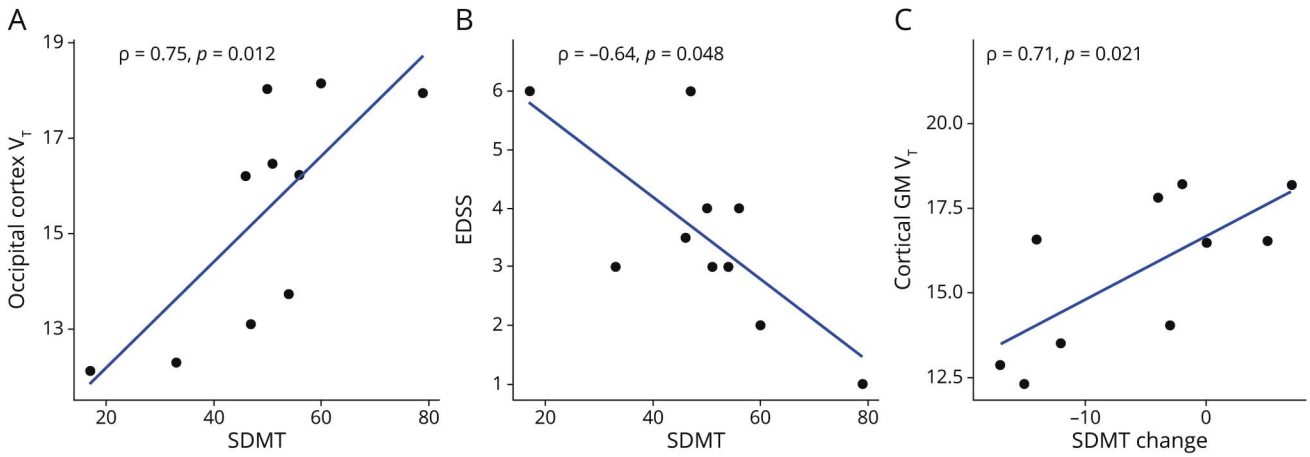

(A) V_T values of the cortex GM in pwMS correlate significantly with SDMT scores. Pearson correlation coefficient was used to evaluate the relationship. (B) In pwMS, EDSS correlates significantly with SDMT scores. Spearman correlation coefficient was used to evaluate the relationship. (C) Illustration of the significant correlation between cortical GM V_T and SDMT change over 5 years before PET imaging. Pearson correlation coefficients were used to evaluate the relationship. *p* Values in the figures are crude without any adjustment. EDSS = Expanded Disability Status Scale; GM = gray matter; pwMS = people with multiple sclerosis; SDMT = Symbol Digit Modalities Test.

However, our investigations have some limitations. First of all, our study cohort was relatively small, which causes susceptibility of the results to the influence of outliers or individual variations. Furthermore, it is important to note that while we can report a correlation between SDMT values and V_T values, we cannot explicitly imply a direct causal relationship between the variables. In our study, the synaptic density was not associated with disease duration or physical disability, nor with preceding physical disability progression. Several reasons might account for that. First, the effect might be too subtle to be measurable in a small cohort. Second, the association might be only with smaller subregions, e.g., the motor cortex, which was not separately analyzed in this study. Finally, EDSS scores are highly affected also by spinal cord pathology, which we could not assess in this study. Furthermore, synaptic loss in the GM is likely not evenly distributed. According to histologic studies, more pronounced synaptic loss takes place in lesional GM. Here, we did not distinguish between myelinated and demyelinated GM areas, which could be valuable to describe more differentiated changes. In addition, the question how different stages of the disease contribute to synaptic loss in MS remains to be answered in further investigations.

Table 3 Correlations of Radiologic and Cognitive Measures of pwMS

V_T of regions	SDMT	SDMT change
Primary regions		
Cortical GM V_T	0.71[a]	0.71[a]
Cingulate cortex V_T	0.71[a]	0.70[a]
Frontal cortex V_T	0.69[a]	0.76[a]
Insular cortex V_T	0.71[a]	0.64[a]
Occipital cortex V_T	0.75[a]	0.67[a]
Parietal cortex V_T	0.74[a]	0.69[a]
Temporal cortex V_T	0.69[a]	0.66[a]
Exploratory regions		
Amygdala V_T	0.76[a]	0.75[a]
Caudate nucleus V_T	0.74[a]	0.69[a]
Cerebellum V_T	0.74[a]	0.63
Hippocampus V_T	0.68[a]	0.72[a]
Putamen V_T	0.56	0.63[a]
Thalamus V_T	0.62	0.75[a]

Abbreviation: FDR = false discovery rate; GM = gray matter; MS = multiple sclerosis; SDMT = Symbol Digit Modalities Test; V_T = distribution volume.
[a] Correlation is significant at $p < 0.05$. Pearson correlation coefficients were calculated to evaluate the relationships because none of the included variables violated the normality assumptions. For primary subregions, all SDMT and SDMT change correlations survived the FDR correction.

Conclusively, we provide with this study evidence of the presence of synaptic loss in pwMS in vivo. We suggest direct involvement of synaptic loss in cognitive dysfunction and in the progression of cognitive disability. Our study underscores the important role of synapse-related pathology in adverse cognitive outcomes and suggests that synaptic density may serve as a promising target for further investigations in the search for suitable biomarkers and predictive measures for the progression of MS.

Acknowledgment

The authors warmly thank all research participants and the staff of the Turku PET Centre for their participation and valuable help in the data collection.

Author Contributions

A. Luoma: drafting/revision of the manuscript for content, including medical writing for content; major role in the acquisition of data; study concept or design; analysis or interpretation of data. M. Matilainen: drafting/revision of the manuscript for content, including medical writing for content; major role in the acquisition of data; study concept or design; analysis or interpretation of data. J.M. Tuisku: drafting/revision of the manuscript for content, including medical writing for content; analysis or interpretation of data. R. Aarnio: drafting/revision of the manuscript for content, including medical writing for content; major role in the acquisition of data; analysis or interpretation of data. T. Nikkilä: major role in the acquisition of data. S. Laaksonen: major role in the acquisition of data. M. Koivumäki: major role in the acquisition of data. E. Honkonen: major role in the acquisition of data. M. Nylund: study concept or design. S. Wahlroos: major role in the acquisition of data. O. Solin: drafting/revision of the manuscript for content, including medical writing for content; analysis or interpretation of data. M-K. Chen: study concept or design. T. Toyonaga: study concept or design. J. Lehto: major role in the acquisition of data. A. Snellman: major role in the acquisition of data. J.O. Rinne: study concept or design. L.M. Airas: drafting/revision of the manuscript for content, including medical writing for content; study concept or design; analysis or interpretation of data.

Study Funding

This study was supported by the Research Council of Finland (decision number: 330902), the InFLAMES Flagship Programme of the Research Council of Finland (decision number 337530), and the US National Multiple Sclerosis Society.

Disclosure

A. Luoma was supported by the Sigrid Juselius Foundation and the InFLAMES Flagship Program of the Research Council of Finland. J. Tuisku was supported by the Finnish Governmental Research Funding (VTR) for Turku University Hospital. S. Laaksonen was support by the Finnish Brain Foundation, Turku Doctoral Program in Clinical Research and VTR for Turku University Hospital. L. Airas has received honoraria from F. Hoffmann-La Roche Ltd., Genzyme, Janssen and Merck Serono and institutional research grant support from the Research Council of Finland, Genzyme, Merck Serono and Novartis. M. Koivumäki, E. Honkonen, M. Nylund, S. Wahlroos, M.-K. Chen, T. Toyonaga, J. Lehto, A. Snellman, J. Rinne, T. Nikkilä, R. Aarnio, and M. Matilainen reports no disclosures. Full disclosure form information provided by the authors is available with the full text of this article at Neurology.org/NN.

Publication History

Received by *Neurology® Neuroimmunology & Neuroinflammation* October 18, 2024. Accepted in final form May 6, 2025. Submitted and externally peer reviewed. The handling editor was Scott S. Zamvil, MD, PhD, FAAN.

References

1. Walton C, King R, Rechtman L, et al. Rising prevalence of multiple sclerosis worldwide: insights from the Atlas of MS, third edition. *Mult Scler*. 2020;26(14):1816-1821. doi:10.1177/1352458520970841
2. Lectures on the diseases of the nervous System. *Br Foreign Med Chir Rev*. 1877;60(119):180-181
3. Benedict RHB, Amato MP, DeLuca J, Geurts JJG. Cognitive impairment in multiple sclerosis: clinical management, MRI, and therapeutic avenues. *Lancet Neurol*. 2020;19(10):860-871. doi:10.1016/S1474-4422(20)30277-5
4. Di Filippo M, Portaccio E, Mancini A, Calabresi P. Multiple sclerosis and cognition: synaptic failure and network dysfunction. *Nat Rev Neurosci*. 2018;19(10):599-609. doi:10.1038/s41583-018-0053-9
5. Calabrese M, Poretto V, Favaretto A, et al. Cortical lesion load associates with progression of disability in multiple sclerosis. *Brain a J Neurol*. 2012;135(Pt 10):2952-2961. doi:10.1093/brain/aws246
6. Möck EEA, Honkonen E, Airas L. Synaptic loss in multiple sclerosis: a systematic review of human post-mortem studies. *Front Neurol*. 2021;12:782599. doi:10.3389/fneur.2021.782599
7. Jürgens T, Jafari M, Kreutzfeldt M, et al. Reconstruction of single cortical projection neurons reveals primary spine loss in multiple sclerosis. *Brain*. 2016;139(Pt 1):39-46. doi:10.1093/brain/awv353
8. Werneburg S, Jung J, Kunjamma RB, et al. Targeted complement inhibition at synapses prevents microglial synaptic engulfment and synapse loss in demyelinating disease. *Immunity*. 2020;52(1):167-182.e7. doi:10.1016/j.immuni.2019.12.004
9. Michailidou I, Willems JGP, Kooi EJ, et al. Complement C1q-C3-associated synaptic changes in multiple sclerosis hippocampus. *Ann Neurol*. 2015;77(6):1007-1026. doi:10.1002/ana.24398
10. Albert M, Barrantes-Freer A, Lohrberg M, et al. Synaptic pathology in the cerebellar dentate nucleus in chronic multiple sclerosis. *Brain Pathol*. 2017;27(6):737-747. doi:10.1111/bpa.12450
11. Petrova N, Nutma E, Carassiti D, et al. Synaptic loss in multiple sclerosis spinal cord. *Ann Neurol*. 2020;88(3):619-625. doi:10.1002/ana.25835
12. Finnema SJ, Nabulsi NB, Eid T, et al. Imaging synaptic density in the living human brain. *Sci Transl Med*. 2016;8(348):348ra96. doi:10.1126/scitranslmed.aaf6667
13. Bartholome O, Van den Ackerveken P, Sánchez Gil J, et al. Puzzling out synaptic vesicle 2 family members functions. *Front Mol Neurosci*. 2017;10:148. doi:10.3389/fnmol.2017.00148
14. Finnema SJ, Nabulsi NB, Mercier J, et al. Kinetic evaluation and test-retest reproducibility of [11C]UCB-J, a novel radioligand for positron emission tomography imaging of synaptic vesicle glycoprotein 2A in humans. *J Cereb Blood Flow Metab*. 2018;38(11):2041-2052. doi:10.1177/0271678X17724947
15. Varrone A, Sjöholm N, Eriksson L, Gulyás B, Halldin C, Farde L. Advancement in PET quantification using 3D-OP-OSEM point spread function reconstruction with the HRRT. *Eur J Nucl Med Mol Imaging*. 2009;36(10):1639-1650. doi:10.1007/s00259-009-1156-3
16. Milicevic SephtonS, Miklovicz T, Russell JJ, et al. Automated radiosynthesis of [11C]UCB-J for imaging synaptic density by positron emission tomography. *J Label Compd Radiopharm*. 2020;63(3):151-158. doi:10.1002/jlcr.3828
17. Rokka J, Schlein E, Eriksson J. Improved synthesis of SV2A targeting radiotracer [^{11}C]UCB-J. *EJNMMI Radiopharm Chem*. 2019;4(1):30. doi:10.1186/s41181-019-0080-5
18. Nabulsi NB, Mercier J, Holden D, et al. Synthesis and preclinical evaluation of 11C-UCB-J as a PET tracer for imaging the synaptic vesicle glycoprotein 2A in the brain. *J Nucl Med*. 2016;57(5):777-784. doi:10.2967/jnumed.115.168179
19. Rokka J, Nordeman P, Roslin S, Eriksson J. A comparative study on Suzuki-type 11C-methylation of aromatic organoboranes performed in two reaction media. *J labelled Compd Radiopharm*. 2021;64(11):447-455. doi:10.1002/jlcr.3932
20. Mansur A, Rabiner EA, Comley RA, et al. Characterization of 3 PET tracers for quantification of mitochondrial and synaptic function in healthy human brain: 18F-BCPP-EF, 11C-SA-4503, and 11C-UCB-J. *J Nucl Med*. 2020;61(1):96-103. doi:10.2967/jnumed.119.228080
21. Karjalainen T, Tuisku J, Santavirta S, et al. Magia: Robust automated image processing and kinetic modeling toolbox for PET neuroinformatics. *Front Neuroinform*. 2020;14:3. doi:10.3389/fninf.2020.00003
22. Fischl B. FreeSurfer. *Neuroimage*. 2012;62(2):774-781. doi:10.1016/j.neuroimage.2012.01.021
23. Schmidt P, Gaser C, Arsic M, et al. An automated tool for detection of FLAIR-hyperintense white-matter lesions in Multiple Sclerosis. *Neuroimage*. 2012;59(4):3774-3783. doi:10.1016/j.neuroimage.2011.11.032
24. Rissanen E, Tuisku J, Vahlberg T, et al. Microglial activation, white matter tract damage, and disability in MS. *Neurol Neuroimmunol Neuroinflamm*. 2018;5(3):e443. doi:10.1212/NXI.0000000000000443
25. Wegner C, Esiri MM, Chance SA, Palace J, Matthews PM. Neocortical neuronal, synaptic, and glial loss in multiple sclerosis. *Neurology*. 2006;67(6):960-967. doi:10.1212/01.wnl.0000237551.26858.39
26. Vercellino M, Marasciulo S, Grifoni S, et al. Acute and chronic synaptic pathology in multiple sclerosis gray matter. *Mult Scler*. 2022;28(3):369-382. doi:10.1177/13524585211022174

27. Vercellino M, Merola A, Piacentino C, et al. Altered glutamate reuptake in relapsing-remitting and secondary progressive multiple sclerosis cortex: correlation with microglia infiltration, demyelination, and neuronal and synaptic damage. *J Neuropathol Exp Neurol*. 2007;66(8):732-739. doi:10.1097/nen.0b013e31812571b0
28. van Olst L, Rodriguez-Mogeda C, Picon C, et al. Meningeal inflammation in multiple sclerosis induces phenotypic changes in cortical microglia that differentially associate with neurodegeneration. *Acta Neuropathol (Berl)*. 2021;141(6):881-899. doi:10.1007/s00401-021-02293-4
29. Kutzelnigg A, Faber-Rod JC, Bauer J, et al. Widespread demyelination in the cerebellar cortex in multiple sclerosis. *Brain Pathol*. 2007;17(1):38-44. doi:10.1111/j.1750-3639.2006.00041.x
30. Howell OW, Schulz-Trieglaff EK, Carassiti D, et al. Extensive grey matter pathology in the cerebellum in multiple sclerosis is linked to inflammation in the subarachnoid space. *Neuropathol Appl Neurobiol*. 2015;41(6):798-813. doi:10.1111/nan.12199
31. Papadopoulos D, Dukes S, Patel R, Nicholas R, Vora A, Reynolds R. Substantial archaeocortical atrophy and neuronal loss in multiple sclerosis. *Brain Pathol*. 2009;19(2):238-253. doi:10.1111/j.1750-3639.2008.00177.x
32. Dutta R, Chang A, Doud MK, et al. Demyelination causes synaptic alterations in hippocampi from multiple sclerosis patients. *Ann Neurol*. 2011;69(3):445-454. doi:10.1002/ana.22337
33. Michailidou I, Willems JGP, Kooi EJ, et al. Complement C1q-C3–associated synaptic changes in multiple sclerosis hippocampus. *Ann Neurol*. 2015;77(6):1007-1026. doi:10.1002/ana.24398
34. Johansen A, Beliveau V, Colliander E, et al. An in vivo high-resolution human brain atlas of synaptic density. *J Neurosci official J Soc Neurosci*. 2024;44(33):e1750232024. doi:10.1523/JNEUROSCI.1750-23.2024
35. Radhakrishnan R, Skosnik PD, Ranganathan M, et al. In vivo evidence of lower synaptic vesicle density in schizophrenia. *Mol Psychiatry*. 2021;26(12):7690-7698. doi:10.1038/s41380-021-01184-0
36. Holmes SE, Scheinost D, Finnema SJ, et al. Lower synaptic density is associated with depression severity and network alterations. *Nat Commun*. 2019;10(1):1529. doi:10.1038/s41467-019-09562-7
37. D'Souza DC, Radhakrishnan R, Naganawa M, et al. Preliminary in vivo evidence of lower hippocampal synaptic density in cannabis use disorder. *Mol Psychiatry*. 2021;26(7):3192-3200. doi:10.1038/s41380-020-00891-4
38. Chen MK, Mecca AP, Naganawa M, et al. Assessing synaptic density in Alzheimer disease with synaptic vesicle glycoprotein 2A positron emission tomographic imaging. *JAMA Neurol*. 2018;75(10):1215-1224. doi:10.1001/jamaneurol.2018.1836
39. Andersen KB, Hansen AK, Damholdt MF, et al. Reduced synaptic density in patients with lewy body dementia: an [11 C]UCB-J PET imaging study. *Mov Disord*. 2021;36(9):2057-2065. doi:10.1002/mds.28617
40. Matuskey D, Tinaz S, Wilcox KC, et al. Synaptic changes in Parkinson disease assessed with in vivo imaging. *Ann Neurol*. 2020;87(3):329-338. doi:10.1002/ana.25682
41. Peterson JW, Bo L, Mork S, Chang A, Trapp BD. Transected neurites, apoptotic neurons, and reduced inflammation in cortical multiple sclerosis lesions. *Ann Neurol*. 2001;50(3):389-400. doi:10.1002/ana.1123
42. Bevan RJ, Evans R, Griffiths L, et al. Meningeal inflammation and cortical demyelination in acute multiple sclerosis. *Ann Neurol*. 2018;84(6):829-842. doi:10.1002/ana.25365
43. Chiaravalloti ND, Stojanovic-Radic J, DeLuca J. The role of speed versus working memory in predicting learning new information in multiple sclerosis. *J Clin Exp Neuropsychol*. 2013;35(2):180-191. doi:10.1080/13803395.2012.760537
44. Rao SM, Leo GJ, Bernardin L, Unverzagt F. Cognitive dysfunction in multiple sclerosis. I. Frequency, patterns, and prediction. *Neurology*. 1991;41(5):685-691. doi:10.1212/wnl.41.5.685
45. López-Góngora M, Querol L, Escartín A. A one-year follow-up study of the Symbol Digit Modalities Test (SDMT) and the Paced Auditory Serial Addition Test (PASAT) in relapsing-remitting multiple sclerosis: an appraisal of comparative longitudinal sensitivity. *BMC Neurol*. 2015;15:40. doi:10.1186/s12883-015-0296-2
46. Morrow SA, Drake A, Zivadinov R, Munschauer F, Weinstock-Guttman B, Benedict RHB. Predicting loss of employment over three years in multiple sclerosis: clinically meaningful cognitive decline. *Clin Neuropsychol*. 2010;24(7):1131-1145. doi:10.1080/13854046.2010.511272
47. Benedict RH, DeLuca J, Phillips G, et al. Validity of the Symbol Digit Modalities Test as a cognition performance outcome measure for multiple sclerosis. *Mult Scler*. 2017;23(5):721-733. doi:10.1177/1352458517690821
48. Kavaliunas A, Tinghög P, Friberg E, et al. Cognitive function predicts work disability among multiple sclerosis patients. *Mult Scler J Exp Transl Clin*. 2019;5(1):2055217318822134. doi:10.1177/2055217318822134
49. Strober LB, Bruce JM, Arnett PA, et al. A much needed metric: defining reliable and statistically meaningful change of the oral version Symbol Digit Modalities Test (SDMT). *Mult Scler Relat Disord*. 2022;57:103405. doi:10.1016/j.msard.2021.103405
50. Silva PHR, Spedo CT, Barreira AA, Leoni RF. Symbol digit modalities test adaptation for magnetic resonance imaging environment: a systematic review and meta-analysis. *Mult Scler Relat Disord*. 2018;20:136-143. doi:10.1016/j.msard.2018.01.014
51. Benedict RHB, Bakshi R, Simon JH, Priore R, Miller C, Munschauer F. Frontal cortex atrophy predicts cognitive impairment in multiple sclerosis. *J Neuropsychiatry Clin Neurosci*. 2002;14(1):44-51. doi:10.1176/jnp.14.1.44